



Vaasan yliopisto  
UNIVERSITY OF VAASA

**OSUVA** Open  
Science

This is a self-archived – parallel published version of this article in the publication archive of the University of Vaasa. It might differ from the original.

## Performance and emissions of a non-road diesel engine driven with a blend of renewable naphtha and diesel fuel oil

**Author(s):** Niemi, Seppo; Hissa, Michaela; Ovaska, Teemu; Sirviö, Katriina; Vauhkonen, Ville

**Title:** Performance and emissions of a non-road diesel engine driven with a blend of renewable naphtha and diesel fuel oil

**Year:** 2019

**Version:** Accepted manuscript

**Copyright** ©2019 Technische Akademie Esslingen

### Please cite the original version:

Niemi, S., Hissa, M., Ovaska, T., Sirviö, K., & Vauhkonen, V., (2019). Performance and emissions of a non-road diesel engine driven with a blend of renewable naphtha and diesel fuel oil. In: Schubert, N., (ed.), *Fuels : conventional and future energy for automobiles: 12th International Colloquium Fuels - Conventional and Future Energy for Automobiles (2019)*, Ostfildern, Deutschland, 25.06.2019 - 26.06.2019. Technische Akademie Esslingen.

# Performance and emissions of a non-road diesel engine driven with a blend of renewable naphtha and diesel fuel oil

Seppo Niemi  
University of Vaasa, Vaasa, Finland

Michaela Hissa  
University of Vaasa, Vaasa, Finland

Teemu Ovaska  
University of Vaasa, Vaasa, Finland

Katriina Sirviö  
University of Vaasa, Vaasa, Finland

Ville Vauhkonen  
UPM-Kymmene Oyj, Lappeenranta, Finland

## Summary

Diesel engines are still the predominant power source in heavy-duty vehicle, non-road, marine and power generation applications globally. They are reliable stand-alone machines with a high brake thermal efficiency (BTE) across a wide output range. Most diesels burn fuel derived from crude oil. However, the share of renewable fuels is growing in response to the need to reduce greenhouse gas emissions (GHG). This study evaluated the suitability of a blend of renewable naphtha (20 vol.-%) and low-sulphur light fuel oil (LFO, 80 vol.-%) for a high-speed, non-road engine. Neat LFO served as the baseline fuel. Wood residue-based hydrotreated vegetable oil (HVO) was the study's third test fuel. With HVO, the engine BTE was a shade higher than with the blend or LFO. HVO also reduced  $\text{NO}_x$  slightly and emitted the lowest HC and the lowest PN within the entire size range of 6 to 560 nm. The blend and LFO showed similar  $\text{NO}_x$  emissions. The blend's HC emissions were higher than LFO's. The blend produced the lowest particle number (PN) of above particles 23 nm: LFO produced the highest. Potent GHG compounds  $\text{CH}_4$  and  $\text{N}_2\text{O}$  were negligible for all three fuels.

## 1. Introduction

Rapid and far-reaching transitions in land, energy, industry, buildings, transport and cities are needed to tackle global warming [1]. Despite significant growth of alternative energy sources, sustainable liquid fuels will be needed for decades to satisfy global growth in energy demands [2].

Electric and hybrid propulsion powertrains are gaining a foothold in the road transport sector but the internal combustion engine (ICE) is likely to dominate, especially in marine, power plant and non-road applications, for a long time. The ICE continues to improve as a result of better combustion, exhaust after-treatment and control systems. New sustainable and renewable fuels are being explored and developed. These fuels help ICE-driven power generation to meet increasingly stringent requirements for local air quality and greenhouse gas (GHG) emissions. [3, 4]. The high brake thermal efficiency (BTE), strength and durability of the ICE fortify

its position as a prime energy producer [5]. The high energy density of liquid fuels is ideal for machines and equipment operating over long periods far from any infrastructure. Furthermore, there is established worldwide distribution of liquid fuels [6].

Several liquid fuel alternatives have been developed during recent decades, and engines have been optimized to use these new fuel options. The sustainability of new fuels depends on many issues, such as land use, cultivation and energy needed for their manufacturing processes, transport and distribution. Alternative fuels derived from waste or residue generally are considered to be the most sustainable [7, 8]. In many respects, hydro treated vegetable oils (HVO) and synthetic fuels produced by the Fischer-Tropsch (FT) process are very suitable for ICE use. HVO fuels are manufactured from a variety of raw materials, such as vegetable oils, animal fat wastes or forest residue.

HVO fuels offer one of the easiest ways to increase the bio-component in diesel fuel. Vehicle and engine manufacturers have also highly recommended their use [9]. HVO is free from sulphur and aromatic compounds. It has a high cetane number (CN) and favourable storage stability [10]. These properties correspond to those of traditional fossil fuels but HVO also offers the bonus of a significant, 80% reduction in GHG emissions [11].

Renewable, wood-based naphtha is another interesting and novel fuel. The naphtha used in this study was a product of HVO manufacture, based on crude tall oil (CTO) extracted during wood pulp production. Colourless, sulphur-free, paraffinic naphtha is chemically pure hydrocarbon and is primarily intended for a bio-component in fossil gasoline [12]. It is more usual for naphtha to be produced from crude oil and it is also suitable for use in compression ignition (CI) engines [13, 14, 15]. However, pure naphtha has a low CN and low viscosity, which may cause increased NO<sub>x</sub> emissions due to the retarded start of combustion and pro-longed ignition delay (ID) [16]. By means of a combustion research unit (CRU), Hissa et al. [17] showed that the neat wood-based naphtha of the present study also had a prolonged ID and retarded start of combustion. Therefore, naphtha was selected to the current study as a blending bio-component in low-sulphur light or diesel fuel oil (LFO).

Fuel characteristics have a significant influence on the emissions and operational safety of an ICE. The increasing requirement to use a variety of renewable fuels demands considerable research into the interaction of those fuels with the engine. Fuel quality affects the composition of diesel exhaust as well as engine performance and durability. Exhaust emissions standards are becoming increasingly stringent. Both neat renewable fuels and blends of renewable and conventional fuels are being studied. Various blends of renewable and conventional fuels provide a fast way to increase the share of sustainable fuels. New fuels should also fulfil the quality assurance and standardization requirements to secure acceptance by consumers [4, 18, 19, 20, 21, 22, 23].

Consequently, the present study focused on evaluating the performance and exhaust emissions of a high-speed, non-road diesel engine, driven with a blend of renewable naphtha and low-sulphur light fuel oil (Naphtha-LFO) and also by neat renewable diesel (HVO). The baseline fuel was neat LFO. The main aim was to analyze combustion, determine BTE and measure gaseous and particle emissions in the exhaust. Unregulated compounds like methane and nitrous oxide were also measured. No engine parameters were optimized at this first stage: all fuels were studied using similar engine settings.

## 2. Experimental setup

### 2.1 Fuels

Both the naphtha and HVO for this study were delivered by UPM, Finland. The naphtha, a product of the HVO manufacturing process, was blended with LFO. This was to ensure the suitability of this low-cetane, low-viscosity fuel for use in the CI test engine. The blend contained 20 vol.-% of naphtha.

The wood residue-based renewable HVO was produced from crude tall oil (CTO). The production process for this CTO-based renewable fuel has several phases. CTO, an organic, water-immiscible liquid from a pulp mill, is purified before it is in contact with hydrogenation catalysts. Impurities are reduced to ppm level or lower to ensure the functionality of the hydrogenation catalysts.

CTO used for HVO production originates from UPM's pulp mills in Finland. Hydrotreatment was carried out in the biorefinery's hydrotreatment unit at a pressure range of 2–12 MPa and at a temperature range of 280–430 °C. The hydrotreated CTO raw fuel contains mid-distillate diesel components in addition to lighter naphtha components which are separated using conventional fractionation methods. Figure 1 illustrates the CTO-based renewable fuel production process.

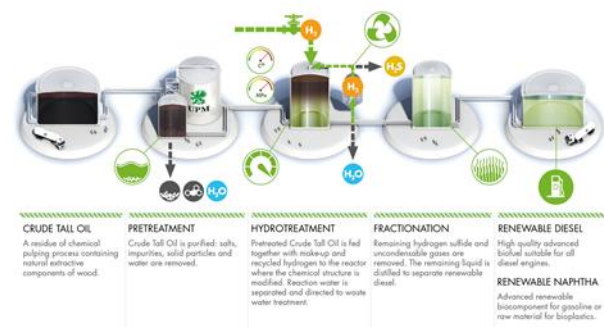


Figure 1. Renewable fuel manufacturing process. Crude tall oil as feedstock.

Neat HVO was used in this study because beneficial results had already been achieved with 100 per cent HVO in a previous test [11]. HVO is free of sulphur and aromatics. Compared with fatty acid methyl esters (FAME), it has a higher CN and better storage stability. HVO also poses fewer problems than FAME in terms of cold operability and deposits [10]. HVO provides the characteristics of fossil fuels but coupled with a reduction of 80% in GHG emissions. Furthermore, production of CTO-derived fuels does not compete with the food chain, and there is no direct land use change. [11]

The fuel analyses came from the fuel suppliers or were carried out by the University of Vaasa's fuel laboratory. Table 1 shows the main specification of the three studied

fuels. Values for the polyaromatics were taken from the literature. The fuel supplier indicated that naphtha may contain negligible traces of polyaromatic compounds. Nevertheless, the polyaromatic content of naphtha-LFO blend was still assumed to meet the SFS-EN 590:2013 standard.

Table 1. Fuel properties.

Parameter	Method	LFO	HVO	Naphtha-LFO
Cetane number	EN 15195	52	65*	51
Density at 15 °C, kg/m <sup>3</sup>	EN ISO 12185/ ASTM D7042	826	813	805
Viscosity at 40 °C, mm <sup>2</sup> /s	EN ISO 3104/ ASTM D7042	1.84	2.85	1.37
Flash point (°C)	ASTM D93-A or C	63	62	10
Sulfur content, mg/kg	EN ISO 20884/ EN ISO 20846	8.3	<5	6.8
Polyaromatics, wt.-%		<8 <sup>a</sup>	0.2 <sup>b</sup>	<8 <sup>a</sup>
Lower heating value, MJ/kg	ASTM D240	43.5	43.7	43.6

\* Cetane index, EN ISO 4264

<sup>a</sup> Maximum allowable polyaromatic content of Standard EN590 [24]

<sup>b</sup> [11]

## 2.2 Engine and dynamometer

The four-cylinder test engine was a turbo-charged, inter-cooled (air-to-water), non-road, diesel engine, equipped with a common-rail fuel-injection system. The engine had no exhaust aftertreatment. The lubricating oil was Valtra Engine CR-4 10W-40. The engine was loaded by means of a Horiba eddy-current dynamometer WT300. The main specification of the engine is in Table 2.

Table 2. Specification of the experimental engine.

Engine	AGCO POWER 44 AWI
Cylinder number	4
Bore (mm)	108
Stroke (mm)	120
Swept volume (dm <sup>3</sup> )	4.4
Rated speed (1/min)	2200
Intermediate speed (1/min)	1500

## 2.3 Analytical instruments

The analytical devices used for the measurements are presented in Table 3: their arrangement and the layout of the test bench are shown in Figure 2.

Sensor data were collected by means of software made in the LabVIEW system-design platform. The recorded

quantities were engine speed and torque, regulated gaseous exhaust emissions, smoke and exhaust particle size distributions. Three unregulated exhaust compounds were also monitored: formaldehyde, methane and nitrous oxide. Several fluid temperatures as well as fluid pressures were also recorded, like the temperatures of cooling water, intake air and exhaust gas plus the pressures of the intake air and exhaust gas.

Table 3. Analytical instruments.

Parameter	Device	Technology
NO <sub>x</sub>	Eco Physics CLD 822 M hr	Chemiluminescence
NO <sub>x</sub> , λ	WDO UniNO <sub>x</sub> sensors	
CO, CO <sub>2</sub>	Siemens Ultramat 6	NDIR
Hydrocarbons	J.U.M. VE7	HFID
O <sub>2</sub>	Siemens Oxymat 61	Paramagnetic
Particle number and size distribution	TSI EEPS 3090	Spectrometer
Smoke	AVL 415 S	Optical filter
Unregulated gaseous emissions	Gasmet DX4000	FTIR
Cylinder pressure, heat release	Kistler KiBox®	
Air mass flow rate	ABB Sensyflow P	Hot-film anemometer

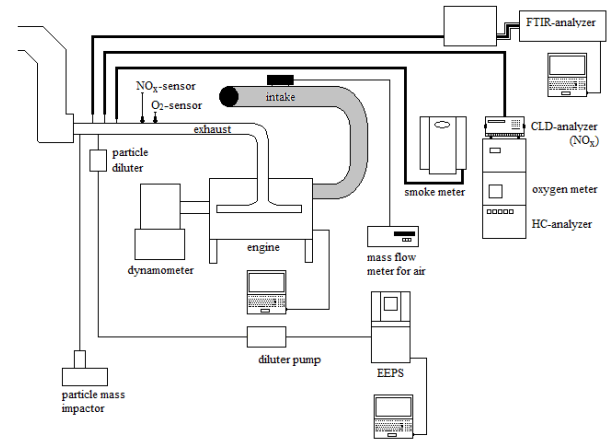


Figure 2. Experimental set-up.

Cylinder pressure was also measured and heat release rates (HRR) were calculated. HRR and the mass fraction of burned fuel (MFB) were computed via a data processing platform of AVL Concerto, using the Thermodynamics2 macro. For HRR, the average values of in-cylinder pressure over 100 consecutive cycles were calculated first. Thereafter, the macro was used to calculate HRR. Finally, the HRR curve was low-pass filtered. For MFB, the cylinder pressures were first filtered before using the macro. The average values of 100 cycles were

not used for MFB to be able to find out the standard deviations.

Particles within a size range of 5.6 to 560 nm were recorded by an EEPS. The sample flow rate was adjusted at 5.0 dm<sup>3</sup>/min. The “SOOT” inversion was applied in the data processing. The exhaust sample was first diluted with ambient air by a rotating disc diluter (RDD) (model MD19-E3, Matter Engineering AG). The dilution ratio used in the RDD was a constant 1:60. The exhaust aerosol sample was conducted to the RDD and dilution air was kept at 150 °C. The diluted sample (5 dm<sup>3</sup>/min) was further diluted by purified air with a dilution ratio of 1:2. Thus, the total dilution ratio was 1:120.

Stable time periods of three minutes were used for the results recordings of the particle number (PN) and size distributions. An averaging interval of two seconds was used for each period. The average PN values, calculated from the recordings, were multiplied by the dilution ratio of the exhaust sample.

The smoke value was an average of three consecutively measured smoke numbers.

The engine control functions were followed via a WinEEM4 program, provided by the engine manufacturer. Engine parameters were not modified and engine settings were kept the same for all fuels. The experimental set-up was precisely the same as in the study of [11].

### 2.3 Experimental matrix and running procedure

The load points or modes of the test cycle C1 of the ISO 8178-4 standard were used in the measurements, Table 4.

Table 4. Experimental matrix.

Mode	1	2	3	4	5	6	7	8
Speed	Rated				Intermediate			Idle
Load, %	100	75	50	10	100	75	50	0
BMEP, bar	10	7.5	5	1	12.9	9.7	6.4	0

Each measurement day, after engine start, warm-up, and up-loading phases, the intake air temperature was adjusted to 100 °C downstream of the charge-air cooler. The temperature was kept constant at all loads. After the completion of each fuel’s measurements, the fuel filter was emptied and the engine was run with the next fuel for 10 minutes. Measurement values were recorded after the engine had stabilized, the criteria being that the temperatures of coolant water, intake air and exhaust were stable. The length of the measurement period was not tied to a certain time. The particle number and size distribution were recorded continuously at each load point. The engine warm-up and measurements procedures were exactly the same for each fuel.

## 3. Results

### 3.1 Combustion analysis

Figure 3 depicts the cylinder pressure at full load at rated speed for each of the three fuels. Due to its high cetane index, HVO most probably ignited earlier than LFO and blend, resulting in a slightly lower maximum cylinder pressure. The pressure traces were, however, very similar indicating an almost equal combustion propagation for all fuels. The highest firing pressure at this load was 110 bar.

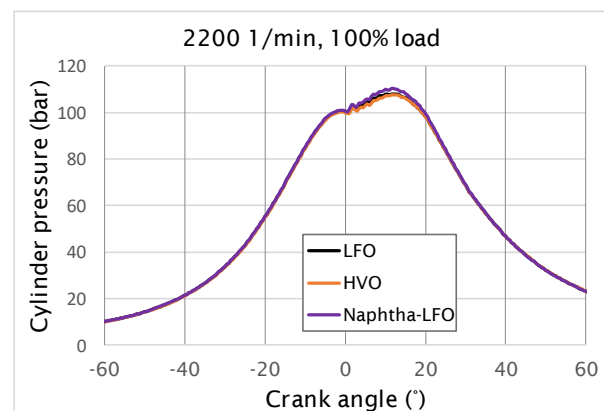


Figure 3. Cylinder pressure against crank angle at 100% load at rated speed for various fuels.

HVO generated a slightly lower peak of premixed combustion, as illustrated in Figure 4 for 75% load at rated speed. This was consistent with HVO’s high cetane index. The heat release rates of each fuel were very similar, although the naphtha-LFO blend seems to show slightly faster burning.

Table 5 lists the crank angles at which 50% of each fuel’s mass was burned at 50% and 75% loads at intermediate speed. The standard deviations of crank angles at MFB50% are also given, calculated from 100 consecutive engine cycles. The results in Table 5 confirm that combustion propagated in a very similar way with all fuels. The cycle-to-cycle variation seemed also to be small.

At 100% and 75% loads at rated speed (Figures 3 and 4), main and post-injection were in use: at 50% and 75% loads at intermediate speed, pilot injections were also adopted.

### 3.2 Efficiency

The engine’s brake thermal efficiency (BTE) was very similar at each load at both speeds with all fuels, Figure 5. HVO usually generated the highest values and the naphtha-LFO blend showed a shade higher BTE than LFO. The results were, however, at all loads within one percentage point and thus of the order of magnitude of

the measuring accuracy. It should be noted that even the highest efficiencies were lower than this engine's typical values. The reason was that the engine was driven at reduced loads to ensure a similar brake torque with all fuels without any modifications of engine settings.

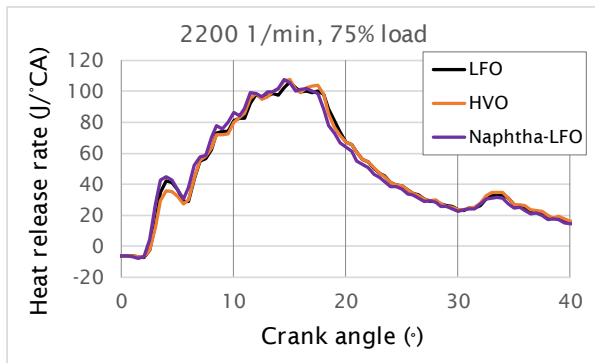


Figure 4. Heat release rates versus crank angle at 75% load at rated speed for different fuels.

Table 5. Average crank angle values and standard deviations for 50% fractions of burned mass of the studied fuels. Crank angles after top dead centre. Standard deviations for 100 consecutive engine cycles.

Load	1500 1/min, 50%		1500 1/min, 75%	
	MFB50%	Stdev	MFB50%	Stdev
Fuel	°CA	°CA	°CA	°CA
LFO	14	0.083	16	0.095
HVO	14	0.084	16	0.093
Naphtha-LFO	14	0.095	15	0.088

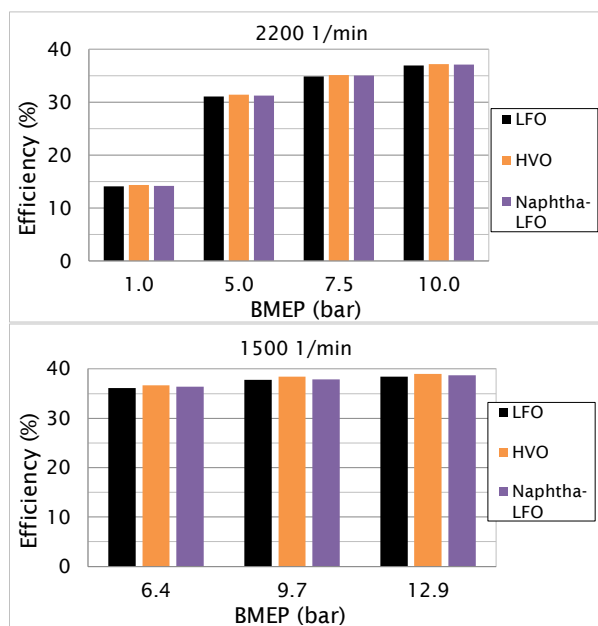


Figure 5. Brake thermal efficiency of the engine against engine load at two speeds for each fuel

### 3.3 Gaseous emissions

Looking at CO first (Figure 6), HVO produced the lowest emissions (0.32 g/kWh) over the measurement cycle. The blend produced the highest (0.36 g/kWh). LFO's CO emissions were 0.33 g/kWh.

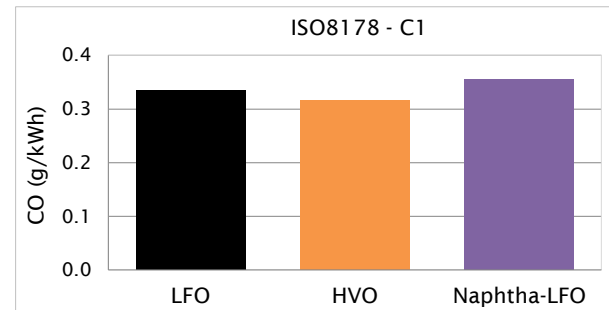


Figure 6. Cycle-weighted carbon monoxide emissions with the studied fuels

Turning to HC emissions (Figure 7), HVO was again the most favourable. Similarly, the naphtha-LFO blend again generated the highest emissions at all loads. Throughout the cycle with weightings, the HC was 0.20 g/kWh for HVO, 0.23 for LFO, and 0.29 g/kWh for the blend.

Unfortunately,  $\text{NO}_x$  values could not be recorded at every load. Therefore,  $\text{NO}_x$  emissions are presented as contents at the highest loads for both engine speeds, Figure 8. The results are comparable since the exhaust flow and engine torque were very similar at those loads for all fuels. At both speeds, HVO showed the lowest  $\text{NO}_x$  contents: 1030ppm (2200 1/min) and 1430 ppm (1500 1/min). At rated speed, LFO generated slightly lower  $\text{NO}_x$  (1080 ppm) than naphtha-LFO blend (1110 ppm). At intermediate speed, the blend showed 1470 ppm and LFO 1480 ppm.

Nitrous oxide contents were very low at all loads, as shown for rated speed in Figure 9. The highest recorded content was approximately 0.6 ppm or within the measuring accuracy of the FTIR analyser. No clear trend was detected and the results were almost equal for all fuels.  $\text{N}_2\text{O}$  generally varied from 0.3 ppm to 0.6 ppm but at full load at intermediate speed it was almost zero.

The wet exhaust contents of methane - another potent greenhouse gas - were also low at all loads, as depicted for rated speed in Figure 10. At higher loads, HVO showed slightly lower  $\text{CH}_4$  contents than naphtha-LFO blend and LFO. At the lowest load, the methane contents from all three fuels were almost equal at 1.8 ppm. There was a clear trend at both engine-speeds: the higher the load, the lower the  $\text{CH}_4$  content. Again, the contents were of the order of magnitude of the measuring accuracy.

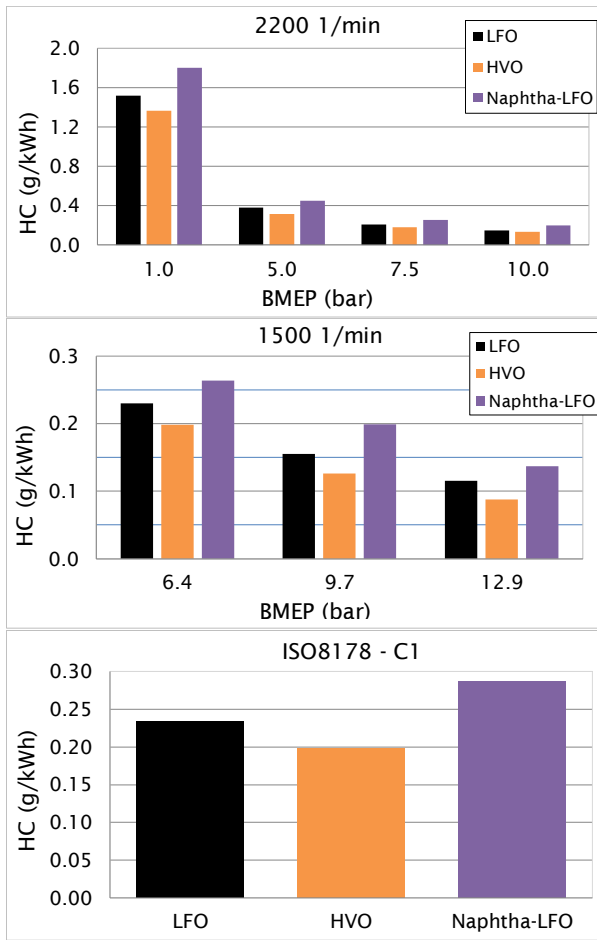


Figure 7. Total hydrocarbons versus engine load at two engine speeds and over the measurement cycle for experimental fuels

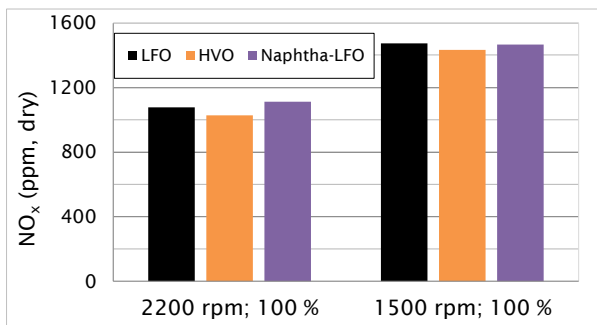


Figure 8. Dry exhaust NO<sub>x</sub> contents at full load at two speeds for all fuels

The wet exhaust formaldehyde contents peaked at 3.0 ppm, as shown for rated speed in Figure 11. At intermediate speed, the CHOH was equal to or lower than 2.0 ppm. No clear trend versus engine load was detected. The differences between fuels were small or negligible. Again, the level of recordings was close to the measuring accuracy.

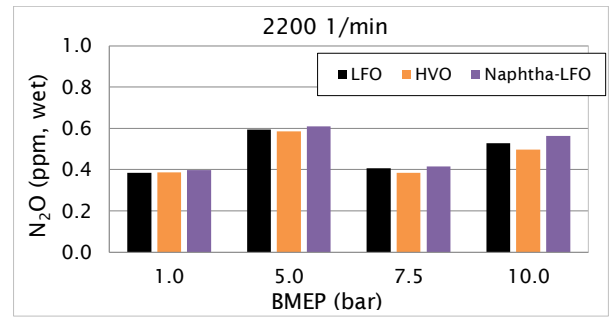


Figure 9. Wet exhaust nitrous oxide contents against engine load at rated speed with the studied fuels

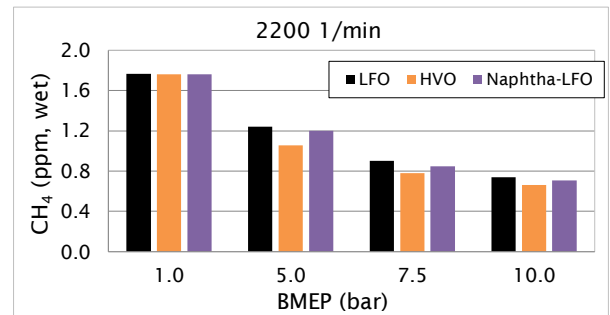


Figure 10. Wet exhaust methane contents versus engine load at rated speed for all fuels

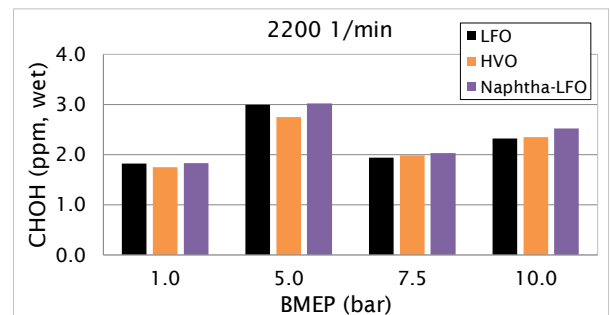


Figure 11. Wet exhaust formaldehyde contents against engine load at rated speed with all fuels.

### 3.4 Particulates and smoke

Figure 12 illustrates two particle size distributions. The upper one was recorded at full load at intermediate speed and the lower at low idle. A bi-modal distribution was detected at high load for all fuels. Only HVO shows a very slight bi-modal distribution at idle. The nucleation mode particles dominated the distributions. HVO generated the lowest nucleation mode particle number (PN) at most loads. At some loads LFO gave the highest nucleation mode PN; at others the highest came from the naphtha-LFO blend.

Figure 13 shows cycle-weighted total PN (TPN) of particles larger than 23 nm. The blend was slightly the most favourable when looking at these particles. TPN was 3% higher with HVO and 12% higher with LFO.

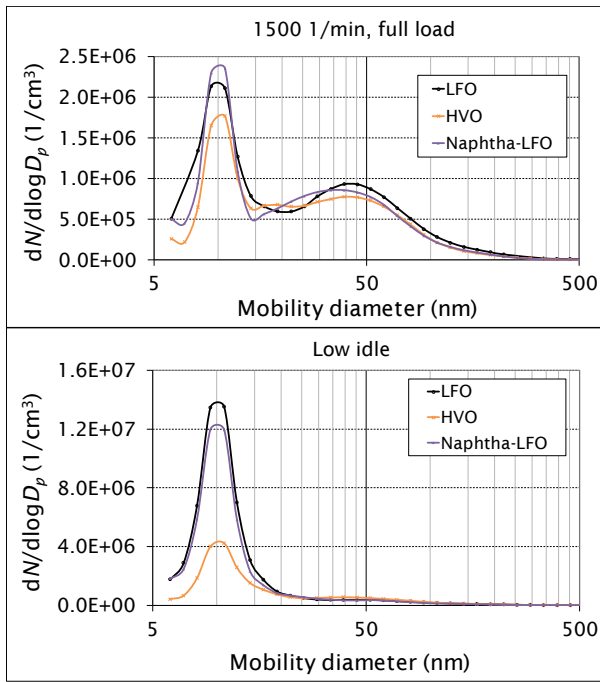


Figure 12. Exhaust particle size distributions at full load at intermediate speed (above) and at low idle for three fuels.

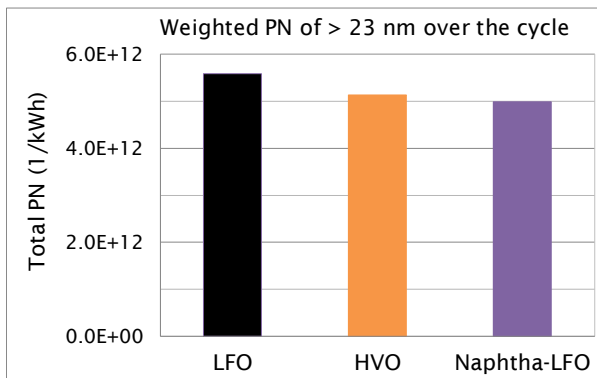


Figure 13. Cycle-weighted total particulate number in the exhaust within the range of 23 to 560 nm for different fuels

This contrasts with the result when looking across the entire size range between 5.6 and 560 nm, as weighted over the measurement cycle. Here, the Naphtha-LFO blend produced the highest TPN: LFO's was 10% lower and HVO's TPN was 20% lower than the blend's.

Smoke was very low. For all fuels, at all loads, it was below 0.04 FSN.

#### 4. Discussion

A liquid fuel's physical properties tend to control its spray characteristics while its composition determines the pathways of chemical reactions during combustion [25]. Most of the physical properties of fuels in this study were very similar. The viscosity of HVO was

slightly higher than that of the blend or LFO but still within a proper range for injection. HVO's cetane index was, however, high. This most probably caused the slightly lower peak of premixed combustion with HVO.

Nevertheless, the combustion performance was very similar for all the tested fuels. The studies of [26, 11] presented similar results for HVO and low-sulphur fossil diesel fuel oil when investigated in passenger car diesel engines and in a non-road diesel engine. Consequently, the engine's BTE throughout the load-speed envelope was very similar with all three fuels.

The high cetane index and lack of polycyclic aromatic compounds of HVO, however, gave this fuel some emissions benefits. Logically, its CO, HC and NO<sub>x</sub> emissions were slightly lower than those from the blend and LFO.

Using naphtha-LFO blend instead of conventional LFO had very little negative effect on emissions performance. However, HC was usually higher. Over the cycle, the blend produced 23% more HC than LFO and 45% more than HVO. The naphtha was a mixture of light hydrocarbons – its distillation range was 20–220 °C [17] – and the lightest hydrocarbons most likely evaporate easily. On one hand, this may have led to improved early combustion. On the other hand, some fractions may have evaporated very quickly, resulting in greater over-leaning compared with HVO and LFO. Over-leaning is one of the most important reasons for increased HC [27].

Levels of sulphur, polyaromatics and ash in a fuel affect emission of particulates. Particle formation is also influenced by other fuel characteristics such as fuel density [28, 29], viscosity [30, 31], and cetane number [32, 33].

Very small nuclei mode particles often dominate the number concentration of particulates, and this was detected in the present study. If it occurs, nucleation usually has a very strong influence on the TPN. Nucleation, condensation and coagulation may change the particle size distribution during the exhaust gas sampling. [34, 35] The exhaust sample was diluted at two stages in this study. According to [36], the nucleation mode evaporates completely when an exhaust sample is heated sufficiently. This study's first dilution used heated air (150 °C) but evidently it was not sufficient to prevent formation of nucleation mode particles.

Problems related to limitations of the measurement systems are avoided by counting only solid particles larger than 23 nm. Unlike the nucleation mode, the accumulation mode is not sensitive to dilution conditions. [37, 38] This solid PN recording procedure allows a reliable measurement of the PN. [35]

This pragmatic approach identified PN benefits for both HVO and naphtha-LFO blend. HVO's favourable PN results were assumed to stem mainly from its very low sulphur and almost zero content of polycyclic aromatic

hydrocarbons. For the blend, the increased share of light, high-volatility hydrocarbons along with naphtha addition most probably improved its TPN performance relative to neat LFO. The blend's lower kinematic viscosity and density also may have served to reduce particle numbers within the size range of 37 to 200 nm relative to LFO.

Safety and feasibility are also critical considerations when new fuels are introduced. Fuel suppliers have to specify fuel properties and confirm compliance with industry standards. One such property is flashpoint: if not properly addressed it jeopardises the safety of personnel or the safe operation of the engine. [39]

The flash point of the naphtha-LFO blend in the present study was low: +10°C. This necessitated additional safety procedures for fuel handling and measurement operations. The engine operators used respirator masks and gloves during the work.

Nevertheless, its low flashpoint will not prevent the use of naphtha-LFO blend in commercial applications. The flashpoint was at the same level as methanol's (+12°C) [40]. Methanol is already successfully used in a ferry, proving that the safety issues of a low flashpoint can be handled in maritime applications. [41]

The next stage of the study should be to optimize the engine control parameters to take greater advantage of individual properties of fuels.

## 5. Conclusions

The primary task of this study was to evaluate how a blend of renewable naphtha (20 vol.-%) and low-sulphur light fuel oil (LFO, 80 vol.-%) suits a high-speed, non-road engine. For comparison, wood residue-based renewable diesel (HVO) was also investigated. Neat LFO served as a baseline fuel. The study comprised combustion analysis, determination of engine efficiency and measurements of the exhaust's gaseous and particle emissions. Based on the performed work, the following conclusions could be drawn:

- The combustion performance was very similar for all fuels. Neat wood residue-based HVO generated a slightly lower peak of pre-mixed combustion. The blend of renewable naphtha and low-sulphur light fuel oil (Naphtha-LFO) seemed to burn fast at an early stage of combustion. The 50% mass fraction burned (MFB) values were, however, found at very similar crank angle positions for all fuels.
- The engine's BTE was very similar for all fuels, but HVO gave a shade higher values at several loads than other fuels.

- HVO usually emitted the lowest regulated exhaust emissions (CO, HC, and NO<sub>x</sub>). LFO showed the next most favourable results. The differences in the three fuels' NO<sub>x</sub> emissions were minor: those for CO slightly clearer. The differences in HC were somewhat larger. The naphtha-LFO blend showed the highest HC emissions, but these were still moderate over the weighted cycle.
- The wet exhaust contents of nitrous oxide, methane and formaldehyde were negligible throughout the load-speed range of the test engine with all fuels.
- Rather high numbers of nuclei-mode particles were measured at several loads. HVO usually showed the lowest PN within this particle size range. However, naphtha-LFO was the most beneficial fuel when considering the total number of particulates larger than 23 nm.
- The flashpoint of naphtha-LFO blend was low, comparable to that of methanol. The use of the blend therefore requires additional safety procedures for fuel handling and storage.
- All in all, naphtha-LFO blend could fuel the non-road test engine without problems. The performance and feasibility of the renewable fuel options must be further improved, however, by optimizing the control parameters and components of the engine.

## Acknowledgements

This study was one part of the EU Hercules-2 programme. The authors express their gratitude to the EU for granting funding for this study. (The European Union's Horizon 2020 research and innovation programme under grant agreement No 634135.) The authors also wish to thank their colleagues Mrs. Sonja Heikkilä, Mr. Olav Nilsson, Mr. Antti Niemi and Ms. Nelli Vanhala for their great contribution during the engine measurement campaign. The Novia University of Applied Sciences allowed us to use the engine laboratory for this study. The authors wish to thank Dr. Tony Pellfolk and Mr. Holger Sved for this possibility.

## References

- [1] IPCC (Intergovernmental Panel on Climate Change), 8<sup>th</sup> October 2018. Press release.
- [2] Alabbad, M., Issayev, G., Badra, J., Voice, A.K., Giri, B.R., Djebbi, K., Ahmed, A., Sarathy, S.M. and Farooq, A. (2018). Autoignition of straight-run naphtha: A promising fuel for advanced compression ignition engines. *Combustion and Flame* 189,

- 337–346. <https://doi.org/10.1016/j.combustflame.2017.10.038>.
- [3] Kalghatgi, G. (2018). Is it really the end of internal combustion engines and petroleum in transport? *Applied Energy* 225, 965–974. <https://doi.org/10.1016/j.apenergy.2018.05.076>.
- [4] Llamas, X., Eriksson, L., (2018), Control-oriented modeling of two-stroke diesel engines with exhaust gas recirculation for marine applications, *Journal of Engineering for the Maritime Environment (Part M)*. <https://doi.org/10.1177/1475090218768992>.
- [5] Gabiña, G., Martin, L., Basurko, O.C., Clemente, M., Aldekoa, S. and Uriondo, Z. (2019). Performance of marine diesel engine in propulsion mode with a waste-oil based alternative fuel, *Fuel* 235, 259–268. <https://doi.org/10.1016/j.fuel.2018.07.113>.
- [6] Hoppe, F., Benedikt, H., Thewes, M., Kremer, F., Pischinger, S., Dahmen, M., Hechinger, M. and Marquardt, W. (2016). Tailor-made fuels for future engine concepts. *International Journal of Engine Research* 17(1), 16–27. <https://doi.org/10.1177/1468087415603005>.
- [7] Schlott, S. (2015). Synthetische Kraftstoffe im Wartestand. *MTZ* 76 6 9–13. (In German.)
- [8] Backhaus, R. (2017). Alternative Kraftstoffe CO<sub>2</sub>-neutral in die Zukunft. *MTZ* 78 6 8–14. (In German.)
- [9] WWFC5 (World Wide Fuel Charter). <http://www.oica.net/wp-content/uploads/WWFC5-2013-Final-single-page-correction2.pdf>. Accessed on January 11, 2019.
- [10] Pirjola, L., Rönkkö, T., Saukko, E., Parviainen, H., Malinen, A., Alanen, J. and Saveljeff, H. (2017). Exhaust emissions of non-road mobile machine: Real-world and laboratory studies with diesel and HVO fuels. *Fuel* 202, 154–164. <https://dx.doi.org/10.1016/j.fuel.2017.04.029>.
- [11] Niemi, S., Vauhkonen, V., Mannonen, S., Ovaska, T., Nilsson, O., Sirviö, K., Heikkilä, S. and Kiijärvi, J. (2016). Effects of wood-based renewable diesel fuel blends on the performance and emissions of a non-road diesel engine. *Fuel* 186, 1–10. <https://dx.doi.org/10.1016/j.fuel.2016.08.048>.
- [12] UPM (2019). Brochure of BioVerno naphtha. <https://www.upmbiofuels.com/products/upm-bi-overno-naphtha/>. Accessed on January 9, 2019.
- [13] Chang, J., Kalghatgi, G., Amer, A., Adomeit, P., Rohs, H. and Heuser, B. (2013). Vehicle Demonstration of Naphtha Fuel Achieving Both High Efficiency and Drivability with EURO6 Engine-Out NO<sub>x</sub> Emission. *SAE International Journal of Engines* 6(1), 101–119. DOI:10.4271/2013-01-0267.
- [14] Wang, X. & Ni, P. (2017). Combustion and emission characteristics of diesel engine fueled with diesel-like fuel from waste lubrication oil. *Energy Conversion and Management* 133, 275–283. <https://doi.org/10.1016/j.enconman.2016.12.018>.
- [15] Bae, C. & Kim, J. (2016). Alternative fuels for internal combustion engines. *Proceedings of the Combustion Institute* 000, 1–25. <http://dx.doi.org/10.1016/j.proci.2016.09.009>.
- [16] Subramanian, T., Varuvel, E., Ganapathy, S., Vedharaj, S. and Vallinayagam, R. (2018). Role of fuel additives on reduction of NO<sub>x</sub> emission from a diesel engine powered by camphor oil biofuel. *Environmental Science and Pollution Research* 25(16), 15368–15377. <https://doi.org/10.1007/s11356-018-1745-4>.
- [17] Hissa, M., Niemi, S. and Sirviö, K. (2018). Combustion property analyses with variable liquid marine fuels in combustion research unit. *Agronomy Research* 16 (S1), 1032–1045, 2018. <https://doi.org/10.15159/AR.18.089>.
- [18] Koch, T., Thee, R. and Maus, W. (2018). Research into Interactions between Internal Combustion Engines and Fuels. *MTZ worldwide*, 01/2018, 50–55.
- [19] Valavanidis, A. (2018). The Shift to Diesel Fuel Engines and How the Emission Scandal of Diesel Vehicles Unfolded. <http://chem-tox-eco-tox.org/Scientificreviews/>. Accessed on February 4, 2018.
- [20] Sirviö, K. 2018. Issues of various alternative fuel blends for off-road, marine and power plant diesel engines. Dissertation. *Acta Wasaensia* 400, University of Vaasa, Finland. <http://urn.fi/URN:ISBN:978-952-476-805-4>.
- [21] Hoseini, S. S., Najafi, G., Ghobadian, B., Mamat, R., Sidik, N. A. C. and Azmi, W. H. (2017). The effect of combustion management on diesel engine emissions fueled with biodiesel-diesel blends. *Renewable and Sustainable Energy Reviews*, 73, 307–331. <https://doi.org/10.1016/j.rser.2017.01.088>.
- [22] Sidhu, M. S., Roy, M. M. and Wang, W. (2018). Glycerine emulsions of diesel-biodiesel blends and their performance and emissions in a diesel engine. *Applied Energy*, 230, 148–159. <https://doi.org/10.1016/j.apenergy.2018.08.103>.

- [23] Lakshminarayanan, A., Olsen, D. B. and Cabot, P. E. (2018). Effects of triglyceride gasoline blends on combustion and emissions in a common rail direct injection diesel engine. *International J of Engine Research*, 19, 1068–1078. Doi:10.1177/1468087417740316.
- [24] SFS-EN 590:2013. Automotive fuels. Diesel. Requirements and test methods. Finnish Petroleum Federation, 2013.
- [25] Eastwood, P. (2008). *Particulate Emissions from Vehicles*. Chichester: John Wiley & Sons Ltd.
- [26] Heuser, B., Vauhkonen, V., Mannonen, S., Rohs, H. and Kolbeck, A. (2013). Crude tall oil-based renewable diesel as a blending component in passenger car diesel engines. *SAE International Journal of Fuels and Lubricants* 6(3):9. <https://www.jstor.org/stable/26273274>.
- [27] Heywood, J. B. (2018). 2<sup>nd</sup> ed. *Internal Combustion Engine Fundamentals*. USA: McGraw-Hill Education. 1028 p.
- [28] Szybist, J. P., Song J., Alam, M. and Boehman, A. L. (2007). Biodiesel combustion, emissions and emission control. *Fuel Process Technol.* 88 (7), 679–691. <https://dx.doi.org/10.1016/j.fuproc.2006.12.008>.
- [29] Bach, F., Tschöke, H. and Simon, H. (2009). Influence of Alternative Fuels on Diesel Engine Aftertreatment. In Bartz, W. J. (ed.): 7<sup>th</sup> International Colloquium Fuels - Mineral oil based and alternative fuels. Ostfildern, Germany: Technische Akademie Esslingen. ISBN 3-924813-75-2.
- [30] Mathis, U., Mohr, M., Kaegi, R., Bertola, A. and Boulouchos K. (2005). Influence of Diesel Engine Combustion Parameters on Primary Soot Particle Diameter. *Environ Sci Technol* 39 (6), 1887–1892. <https://dx.doi.org/10.1021/es049578p>.
- [31] Tsolakis, A. (2006). Effects on Particle Size Distribution from the Diesel Engine Operating on RME-Biodiesel with EGR. *Energy & Fuels* 20 (4), 1418–1424. <https://dx.doi.org/10.1021/ef050385c>.
- [32] Li, R., Wang, Z., Ni, P., Zhao, Y., Li, M. and Li, L. (2014). Effects of cetane number improvers on the performance of diesel engine fuelled with methanol/biodiesel blend. *Fuel* 128, 180–187. <https://dx.doi.org/10.1016/j.fuel.2014.03.011>.
- [33] Alrefaai, M. M., Peña, G. D. G., Raj, A., Stephen, S., Anjana, T. and Dindi, A. (2018). Impact of dicyclopentadiene addition to diesel on cetane number, sooting propensity, and soot characteristics. *Fuel* 216, 110–120. <http://dx.doi.org/10.1016/j.fuel.2017.11.145>.
- [34] Barrios, C. C., Domínguez-Sáez, A., Rubio, J. R. and Pujadas, M. (2011). Development and evaluation of on-board measurement system for nanoparticle emissions from diesel engine. *Aerosol Sci Technol* 45 (5), 570–580. <https://doi.org/10.1080/02786826.2010.550963>.
- [35] Burtscher, H. and Majewski, W. A. (2019). Particulate Matter Measurements. Available at [https://www.dieselnet.com/tech/measure\\_dpm.php](https://www.dieselnet.com/tech/measure_dpm.php). Accessed on March 8, 2019.
- [36] Vaaraslahti, K., Virtanen, A., Ristimäki, J. and Keskinen, J. (2004). Nucleation mode formation in heavy-duty diesel exhaust with and without a particulate filter. *Environ Sci Technol* 38 (18), 4884–4890. <https://dx.doi.org/10.1021/es0353255>.
- [37] Maricq, M. M., Chase, R. E., Xu, N. and Laing, P. M. (2002). The Effects of the Catalytic Converter and Fuel Sulfur Level on Motor Vehicle Particulate Matter Emissions: Light Duty Diesel Vehicles. *Environ Sci Technol* 36 (2), 283–289. DOI:10.1021/es010962l.
- [38] Kittelson, D. B., Watts, W. and Johnson, J. (2002). *Diesel aerosol sampling methodology; CRC E-43 Final Report*. Minneapolis: University of Minnesota.
- [39] International Association of Classification Societies (IACS) (2018). Fuel oil safety considerations associated with the January 2020 0.50% Sulphur cap requirement. Position paper.
- [40] Safety data sheet, Methanol, Lab Grade, 4L. 01.08.2015, 8 pages. Available at [https://beta-static.fishersci.com/content/dam/fishersci/en\\_US/documents/programs/education/regulatory-documents/sds/chemicals/chemicals-m/S25426A.pdf](https://beta-static.fishersci.com/content/dam/fishersci/en_US/documents/programs/education/regulatory-documents/sds/chemicals/chemicals-m/S25426A.pdf).
- [41] Stena Germanica's methanol conversion. Stena Line. Available at <https://www.stenalinefreight.com/news/Methanol-project>. Accessed on February 20, 2019.